

Macroscopic Quantum Entanglement of a Kondo Cloud at Finite Temperature

S.-S. B. Lee, Jinhong Park, and H.-S. Sim*

Department of Physics, Korea Advanced Institute of Science and Technology, Daejeon 305-701, Korea

We propose a variational approach for computing the macroscopic entanglement in a many-body *mixed* state, based on entanglement witness operators, and compute the entanglement of formation (EoF), a mixed-state generalization of the entanglement entropy, in single- and two-channel Kondo systems at finite temperature. The thermal suppression of the EoF obeys power-law scaling at low temperature. The scaling exponent is halved from the single- to the two-channel system, which is attributed, using a bosonization method, to the non-Fermi liquid behavior of a Majorana fermion, a “half” of a complex fermion, emerging in the two-channel system. Moreover, the EoF characterizes the size and power-law tail of the Kondo screening cloud of the single-channel system.

PACS numbers: 75.20.Hr, 03.67.Mn, 72.15.Qm, 71.10.Hf

Systems of many interacting particles often exhibit unusual macroscopic phenomena at zero temperature. A useful concept of understanding their quantum nature is macroscopic entanglement [1, 2], quantum correlation of many particles that cannot be imitated by classical correlations [3]. A popular measure for this purpose is entanglement entropy (EE). It captures entanglement between two macroscopic subsystems, and quantifies new aspects of many-body ground states, including area law [4], topological order [5, 6], and quantum criticality [7, 8].

Generalizing this zero-temperature study is desirable, to explore how the macroscopic entanglement thermally decays or spatially extends. This requires to study a *mixed* state, in which quantum and classical correlations coexist. At finite temperature, a system is in a probabilistic mixture of energy eigenstates. Its entanglement will reveal quantumness in quantum-to-classical crossover, collective excitations, decoherence, etc. Moreover, EE measures entanglement only between two complementary subsystems in a pure state [1], providing limited information about the spatial extension of macroscopic entanglement. To get more direct information, it is useful to consider, e.g., two distant *non-complementary* subsystems with changing the distance, which are described by a mixed state, after the remainder is traced out of a ground or thermal mixed state.

The computation of macroscopic entanglement in many-body mixed states, however, requires huge costs. For mixed states, EE unpredictably overestimates entanglement, since it cannot distinguish between quantum and classical correlations. Thus EE is generalized [9] into the entanglement of formation (EoF) \mathcal{E}_F . EoF quantifies the entanglement between two complementary subsystems A and B of a *mixed* state ρ as

$$\mathcal{E}_F(\rho) = \inf_{\rho = \sum_i p_i |\psi_i\rangle\langle\psi_i|} \left[\sum_i p_i \mathcal{E}_E(|\psi_i\rangle) \right]. \quad (1)$$

It is obtained by exploring the possible decompositions of ρ into normalized pure states $|\psi_i\rangle$ with

weight p_i , and finding the optimal decomposition for which $\sum_i p_i \mathcal{E}_E(|\psi_i\rangle)$ is the lowest. Here, $\mathcal{E}_E(|\psi_i\rangle) \equiv -\text{Tr}(\rho_A \log_2 \rho_A)$ is the EE of $|\psi_i\rangle$ between A and B, and $\rho_A = \text{Tr}_B |\psi_i\rangle\langle\psi_i|$ is obtained from $|\psi_i\rangle$ by tracing out B. For pure states $|\psi\rangle$, EoF reduces to EE, $\mathcal{E}_F(|\psi\rangle) = \mathcal{E}_E(|\psi\rangle)$. The computational cost of exploring the decompositions is huge even for a small system of a three-qubit full-rank state, equivalent to that of minimizing a function of $63 \sim 959$ variables [10–12], and it exponentially increases with system size [13, 14]. Most entanglement measures require such heavy costs [13, 15]. Negativity [16–20] is an exception, however, cannot detect bound entanglement [3, 13] that can appear in many-body systems [21, 22]. Mutual information [3] is not applicable to mixed-state entanglement, as it cannot distinguish between quantum and classical correlations.

On the other hand, in Kondo effects [23], the ground states have the entanglement between the Kondo impurity spin and the surrounding conduction electrons, the latter forming Kondo cloud [24–26]. Naturally, macroscopic entanglement would be a direct tool for characterizing the properties of the cloud, the essence of Kondo effects, that cannot be captured by few-particle correlations [27, 28]. For example, it will be meaningful to characterize the tail of the cloud by macroscopic entanglement, since the tail is expected to reflect the universality of low-energy Kondo physics in real space [25]. Moreover, since Kondo effects have gapless excitations at any low temperature, it is important to study, by macroscopic entanglement, not only their ground state but also their thermal suppression. However, the understanding of the macroscopic entanglement remains unsatisfactory due to the computation difficulty mentioned above, despite efforts [18, 19, 29, 30].

In this Letter, we propose a variational approach for computing macroscopic entanglement in mixed states, based on entanglement witness operators (EWs) [11–13, 31–33], and develop it for single- (1CK) and two-channel Kondo (2CK) systems, using numerical renormalization group (NRG) methods [34, 35]. We compute the EoF \mathcal{E}_F between the impurity and the electrons located within distance L from the impurity at temperature T ; see Fig. 1. In addition to the expected

* Corresponding author. hssim@kaist.ac.kr

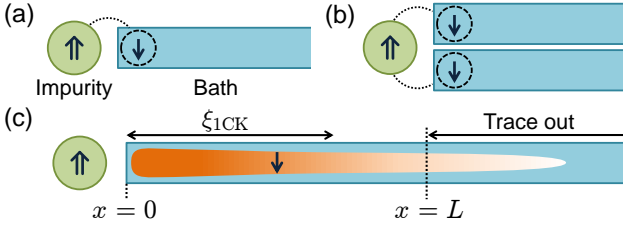


FIG. 1. (Color Online) (a) Single- (1CK) and (b) two-channel Kondo (2CK) systems. In 1CK (2CK), a spin-1/2 impurity is antiferromagnetically coupled with the spin(s) of a single (two) channel(s) of a conduction electron bath at the impurity site [23, 37]; we consider a one-dimensional semi-infinite bath, without loss of generality. (c) In 1CK, the Kondo cloud, a macroscopic electronic object of size $\xi_{1\text{CK}}$, forms to screen the impurity spin at zero temperature. The cloud spin (\uparrow, \downarrow) entangles with the impurity spin (\uparrow, \downarrow), forming the Kondo singlet of the Bell-state type $|\uparrow\downarrow\rangle - |\downarrow\uparrow\rangle$. The entanglement of formation \mathcal{E}_F between the impurity at $x = 0$ and the bath electrons inside distance L ($x \leq L$) quantifies how the macroscopic entanglement of the cloud spatially extends. \mathcal{E}_F is reduced from the value of $L \rightarrow \infty$, if the entanglement between electrons outside L (which are traced out) and the rest exists.

crossover around the Kondo temperature $T_{1\text{CK}(2\text{CK})}$ of 1CK (2CK), the macroscopic entanglement measured by \mathcal{E}_F exhibits, at low temperature, the universal power-law thermal decay of $\mathcal{E}_F \simeq 1 - a_1(T/T_{1\text{CK}})^2$ for 1CK and $\mathcal{E}_F \simeq 1 - a_2T/T_{2\text{CK}}$ for 2CK; $a_{1,2}$ are constants. The halving of the power-law exponent from 1CK to 2CK is attributed, using bosonization methods [36], to a Majorana fermion emerging in 2CK. Moreover, for 1CK, the dependence of \mathcal{E}_F on L characterizes the spatial profile of the Kondo cloud. The cloud size is $\xi_{1\text{CK}} = \hbar v_F/k_B T_{1\text{CK}}$ and robust against thermal effects at $T \lesssim T_{1\text{CK}}$, while it decreases with increasing T at $T \gtrsim T_{1\text{CK}}$; v_F is Fermi velocity. At $T = 0$, the cloud tail obeys another power law, $\mathcal{E}_F \simeq 1 - b_1(\xi_{1\text{CK}}/L)$; b_1 is a constant. The different exponents of 1CK imply that the T and L dependences of \mathcal{E}_F have separate informations about entanglement in thermal states and the spatial extension of entanglement.

Variational approach.— EWs are the physical operators detecting whether a state is entangled [3, 13]. They have been applied for quantifying entanglement in a few particles [11, 12, 31–33]. Here we suggest to use EWs to efficiently compute *macroscopic* entanglement.

We introduce how to compute the EoF $\mathcal{E}_F(\rho)$ of a target state ρ by EW. One finds the set \mathbb{M}_ρ of EWs X , whose expectation value provides a lower bound of $\mathcal{E}_F(\rho)$ as $\text{Tr} X \rho \leq \mathcal{E}_F(\rho)$. Here, $\mathbb{M}_\rho \equiv \{X | \langle \psi | X | \psi \rangle \leq \mathcal{E}_F(|\psi\rangle), \forall |\psi\rangle \in \mathcal{H}_\rho\}$ and a Hilbert space \mathcal{H}_ρ includes the range of ρ . Among X 's, the optimal EW [31, 32] of the largest expectation value provides $\mathcal{E}_F(\rho)$,

$$\mathcal{E}_F(\rho) = \sup_{X \in \mathbb{M}_\rho} \text{Tr} X \rho. \quad (2)$$

It is equivalent to Eq. (1), and the cost of exploring all operators in \mathbb{M}_ρ is huge. Because of the difficulty in

Eqs. (1) and (2), macroscopic entanglement in a thermal many-body state remains unexplored.

In our approach, instead of fully exploring \mathbb{M}_ρ , we construct an appropriate variational form of EW, which covers only a small subset of \mathbb{M}_ρ but includes or is close to the optimal EW. Within the form, we find the operator X_ρ^{opt} whose expectation value $\text{Tr} X_\rho^{\text{opt}} \rho$ is the largest.

A lower bound of $\mathcal{E}_F(\rho)$ is obtained as $\text{Tr} X_\rho^{\text{opt}} \rho$, because X_ρ^{opt} is an EW. We obtain an upper bound by finding a pure-state decomposition of ρ , based on the duality [11, 12]: The optimal decomposition of ρ in Eq. (1) is a mixture of the pure states in a set $\mathbb{P}_X \equiv \{|\psi\rangle | \langle \psi | X | \psi \rangle = \mathcal{E}_F(|\psi\rangle)\}$, if and only if $\text{Tr} X \rho = \mathcal{E}_F(\rho)$ in Eq. (2). We obtain $\mathbb{P}_{X_\rho^{\text{opt}}}$ and search a decomposition of $\rho = \sum_i p'_i |\psi'_i\rangle \langle \psi'_i|$, each $|\psi'_i\rangle$ being sufficiently similar to an element of $\mathbb{P}_{X_\rho^{\text{opt}}}$ [37]. Then, $\sum_i p'_i \mathcal{E}_F(|\psi'_i\rangle)$ is an upper bound. The upper and lower bounds are close together (hence to the exact value) when X_ρ^{opt} is “good”. A good variational form can be constructed for a system at low temperature, considering its ground states and low-energy excitations, as shown below.

EW in Kondo models.— We further develop this approach for Kondo systems; see Fig. 1. Their Hamiltonian is $H = J \sum_\alpha \vec{S} \cdot \vec{s}_\alpha + \sum_{\alpha k \sigma} \epsilon_k c_{\alpha k \sigma}^\dagger c_{\alpha k \sigma}$. J is the coupling strength between the impurity spin \vec{S} and the electron spin $\vec{s}_\alpha = \sum_{kk'\sigma\sigma'} c_{\alpha k \sigma}^\dagger \vec{\sigma}_{\sigma\sigma'} c_{\alpha k' \sigma'}/2$ in channel $\alpha \in [1, M]$ at the impurity site ($x = 0$), $M = 1$ (2) for 1CK (2CK), $\vec{\sigma}$ is Pauli matrix, $c_{\alpha k \sigma}^\dagger$ creates an electron with spin σ , momentum k , and energy ϵ_k in channel α [37].

To compute the EoF, we obtain the state ρ , by building thermal states by NRG [34, 35] and by tracing out the subsystem outside L . We develop a way for the latter within NRG [37]. The resulting ρ generally has rank $\sim 10^4$ too high to exactly obtain $\mathcal{E}_F(\rho)$.

At $T = 0$ and $L \rightarrow \infty$, we exactly obtain optimal EWs based on our derivation [37] of the optimal EW $X_{2\text{qb}}$ for a general two-qubit state $\rho_{2\text{qb}}$, which provides the value of $\mathcal{E}_F(\rho_{2\text{qb}}) = \text{Tr} X_{2\text{qb}} \rho_{2\text{qb}}$ and satisfies $\langle \psi | X_{2\text{qb}} | \psi \rangle \leq \mathcal{E}_F(|\psi\rangle)$ for any pure state $|\psi\rangle$. The 1CK ground state (so-called Kondo singlet), $|G_{1\text{CK}}\rangle = \frac{1}{\sqrt{2}}(|\uparrow\rangle|g_{-1/2}\rangle - |\downarrow\rangle|g_{1/2}\rangle)$, is a two-qubit Bell state of maximal entanglement ($\mathcal{E}_F = 1$) between impurity spin states $|\eta\rangle = \uparrow, \downarrow$ and bath states $|g_{N_s}\rangle$ of spin- z quantum number N_s , satisfying $\langle g_{N_s} | g_{N'_s} \rangle = \delta_{N_s N'_s}$. The optimal EW for $\mathcal{E}_F(|G_{1\text{CK}}\rangle)$ has the form

$$X_{G1} = \frac{2}{\log 2} |G_{1\text{CK}}\rangle \langle G_{1\text{CK}}| - \left(\frac{2}{\log 2} - 1 \right) I_{G1}, \quad (3)$$

where $I_{G1} = \sum_{\eta=\uparrow, \downarrow, N_s=\pm 1/2} |\eta\rangle \langle \eta| \otimes |g_{N_s}\rangle \langle g_{N_s}|$ is the identity operator of the two-qubit Hilbert subspace for $|G_{1\text{CK}}\rangle$. Notice $\langle G_{1\text{CK}} | X_{G1} | G_{1\text{CK}} \rangle = \mathcal{E}_F(|G_{1\text{CK}}\rangle) = 1$.

The two-fold degenerate ground states of 2CK are also two-qubit Bell states ($\mathcal{E}_F = 1$), $|G_{2\text{CK}}^+\rangle = \frac{1}{\sqrt{2}}(|\uparrow\rangle|g_0^+\rangle + |\downarrow\rangle|g_1^+\rangle)$ and $|G_{2\text{CK}}^-\rangle = \frac{1}{\sqrt{2}}(|\uparrow\rangle|g_{-1}^- \rangle + |\downarrow\rangle|g_0^- \rangle)$, where $|G_{2\text{CK}}^\pm\rangle$ has the total spin- z quantum number of $\pm 1/2$ and

$|g_{N_s}^\pm\rangle$ is the bath state associated with $|G_{2\text{CK}}^\pm\rangle$, satisfying $\langle g_{N_s}^p | g_{N_s'}^{p'} \rangle = \delta_{pp'} \delta_{N_s N_s'}$. Thus the 2CK state at $T = 0$ and $L \rightarrow \infty$ is $\rho_{G2} = (|G_{2\text{CK}}^+\rangle\langle G_{2\text{CK}}^+| + |G_{2\text{CK}}^-\rangle\langle G_{2\text{CK}}^-|)/2$. The optimal EW $X_{G2} = X_{G2+} + X_{G2-}$ provides the value of $\mathcal{E}_F(\rho_{G2}) = \text{Tr} X_{G2} \rho_{G2} = 1$, where $X_{G2\pm} = [2|G_{2\text{CK}}^\pm\rangle\langle G_{2\text{CK}}^\pm| - (2 - \log 2)I_{G2\pm}]/\log 2$ and $I_{G2\pm}$ (I_{G2-}) is the identity of two-qubit subspace $\mathcal{H}_{G2+} = \{|\uparrow\rangle, |\downarrow\rangle\} \otimes \{|g_0^+\rangle, |g_1^+\rangle\}$ ($\mathcal{H}_{G2-} = \{|\uparrow\rangle, |\downarrow\rangle\} \otimes \{|g_{-1}^-\rangle, |g_0^-\rangle\}$).

For the state ρ at general T and L , we construct an EW X variationally, generalizing X_{G1} and X_{G2} , as follows. (i) Decompose the whole Hilbert space into two-qubit subspaces $\mathcal{H}_i = \{|\uparrow\rangle, |\downarrow\rangle\} \otimes \{|\phi_{i\uparrow}\rangle, |\phi_{i\downarrow}\rangle\}$, where $\{|\phi_{i\eta}\rangle\}$ is an orthonormal basis of bath states. We parametrize $|\phi_{i\eta}\rangle$'s for the optimization discussed below. (ii) For each subspace \mathcal{H}_i , we obtain the optimal EW X_i which provides $\mathcal{E}_F(\rho_i) = \text{Tr} X_i \rho_i$. Here $\rho_i = I_i \rho I_i$ is the projection of ρ onto \mathcal{H}_i and I_i is the identity of \mathcal{H}_i . This construction of X_i depends on the choice of $\{|\phi_{i\eta}\rangle\}$. (iii) The sum $X = \sum_i X_i$ of the two-qubit EWs is our variational form. We optimize the choice of $\{|\phi_{i\eta}\rangle\}$ (hence X), to make the lower and upper bounds of $\mathcal{E}_F(\rho)$ closer [37].

For example, at $T \ll T_{1\text{CK}, 2\text{CK}}$ and $L \rightarrow \infty$, ρ (for any of 1CK and 2CK) is a mixture of energy eigenstates $|E_i\rangle$ with energy $E_i \ll k_B T_{1\text{CK}, 2\text{CK}}$. $|E_i\rangle = b_{i\uparrow}|\uparrow\rangle|e_{i\uparrow}\rangle + b_{i\downarrow}|\downarrow\rangle|e_{i\downarrow}\rangle$ has an analogous form ($\mathcal{E}_F \lesssim 1$) to the Bell state, where $b_{i\eta} \simeq 1/\sqrt{2}$, $\langle e_{i\eta} | e_{i'\eta'} \rangle = \delta_{\eta\eta'}$, and $\langle e_{i\eta} | e_{i' \neq i, \eta'} \rangle \simeq 0$. Hence we choose $\{|\phi_{i\eta}\rangle\}$ by orthonormalizing $\{|e_{i\eta}\rangle\}$ and construct X_i 's similarly to Eq. (3).

A lower bound of $\mathcal{E}_F(\rho)$ is obtained as $\text{Tr}(\sum_i X_i \rho)$. A upper bound is $\sum_j p'_j \mathcal{E}_F(|\psi'_j\rangle)$, by finding $|\psi'_j\rangle$ which is similar to a state in \mathbb{P}_X and satisfies $\sum_j p'_j |\psi'_j\rangle\langle\psi'_j| = \rho$; to avoid the huge cost of obtaining \mathbb{P}_X , we use a subset $\bigcup_i \mathbb{P}_{X_i} \subset \mathbb{P}_X$. To get better bounds, we optimize the choice of $\{|\phi_{i\eta}\rangle\}$ and $\{p'_j, |\psi'_j\rangle\}$, based on the structure of ρ [37]. X cannot detect off-diagonal blocks $I_i \rho I_{i' \neq i}$ which are however made small at $T \ll T_{1\text{CK}}$ and $L \gg \xi_{1\text{CK}}$ by appropriately choosing $\{|\phi_{i\eta}\rangle\}$. We emphasize that the decomposition into the two-qubit subspaces allows us to avoid the impractical cost of computing EoF by Eq. (1).

Result. — We discuss the result of the temperature dependence of \mathcal{E}_F at $L \rightarrow \infty$ in Fig. 2. In both 1CK and 2CK, \mathcal{E}_F shows maximal entanglement at $T = 0$, slowly decays with $T \lesssim T_{1\text{CK}, 2\text{CK}}$, and rapidly vanishes at $T \gtrsim T_{1\text{CK}, 2\text{CK}}$, exhibiting the crossover around $T_{1\text{CK}, 2\text{CK}}$. At $T \ll T_{1\text{CK}, 2\text{CK}}$, the upper and lower bounds show the same universal power-law decay in each system,

$$\begin{aligned} \mathcal{E}_F &\simeq 1 - a_1 (T/T_{1\text{CK}})^2 & (1\text{CK}), \\ \mathcal{E}_F &\simeq 1 - a_2 (T/T_{2\text{CK}}) & (2\text{CK}). \end{aligned} \quad (4)$$

In Eq. (4), the scaling exponent is halved from 1CK to 2CK, reflecting different low-energy excitations. At $T \ll T_{1\text{CK}, 2\text{CK}}$, the thermal state $\rho = \sum_i w_i |E_i\rangle\langle E_i|$ is governed by $|E_i\rangle$'s with $E_i \simeq k_B T$, because of the competition between Boltzmann weight w_i and degeneracy. There are two sources suppressing $\mathcal{E}_F(\rho)$: (i) Each $|E_i\rangle$ is less entangled; $\mathcal{E}_F(|E_i\rangle) \simeq 1 - 2|S_{z,ii}|^2/\log 2$ for $E_i \ll k_B T_{1\text{CK}, 2\text{CK}}$, where S_z is the impurity spin- z operator

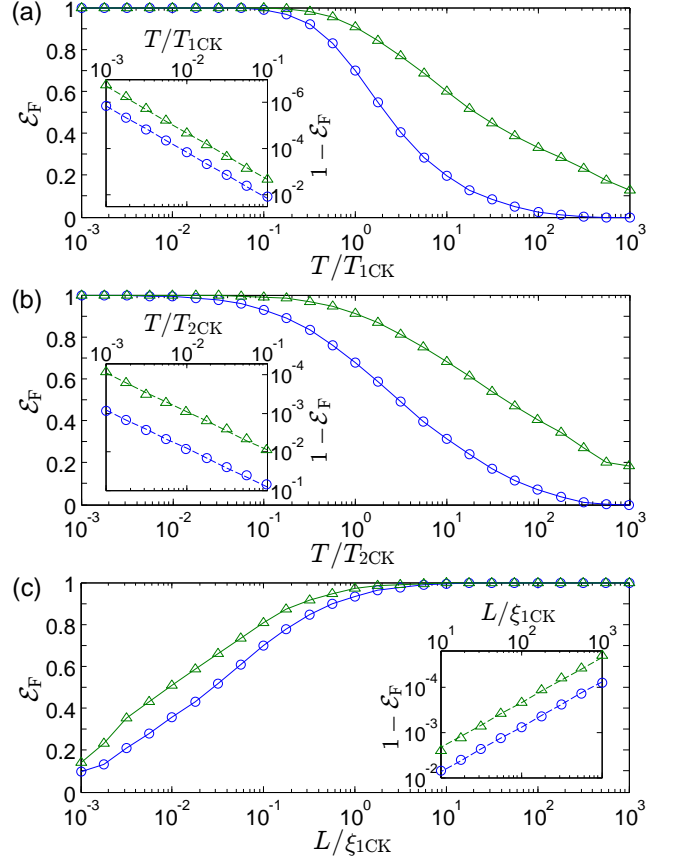


FIG. 2. (Color Online) Entanglement of formation \mathcal{E}_F between the Kondo impurity and the bath electrons inside L at temperature T for single- (1CK) and two-channel Kondo (2CK) systems. (a,b) \mathcal{E}_F versus T at $L \rightarrow \infty$ for (a) 1CK and (b) 2CK. (c) \mathcal{E}_F versus L at $T = 0$ for 1CK. Blue circles (green triangles) denote the lower (upper) bounds of \mathcal{E}_F . These bounds are close to each other, especially at $T < T_{1\text{CK}, 2\text{CK}}$ and $L > \xi_{1\text{CK}}$, enough to predict scaling behavior. Insets: The universal scaling behavior of \mathcal{E}_F versus $T/T_{1\text{CK}, 2\text{CK}} \ll 1$ or $L/\xi_{1\text{CK}} \gg 1$, well fitted by power laws (dashed lines); see Eqs. (4) and (5). The NRG parameters used for this plot and the expression of $T_{1\text{CK}, 2\text{CK}}$ are given in Ref. [37].

and $S_{z,ii} = \langle E_i | S_z | E_i \rangle = (|b_{i\uparrow}|^2 - |b_{i\downarrow}|^2)/2$. (ii) EoF satisfies the convexity, $\mathcal{E}_F(\sum_i w_i |E_i\rangle\langle E_i|) \leq \sum_i w_i \mathcal{E}_F(|E_i\rangle)$. Using bosonization [36], we find that these two sources give the same exponent [37]. Here we explain the former factor. A pseudofermion operator $c^{(\dagger)}$ describes the impurity spin as $S_z = c^\dagger c - 1/2$. In 1CK, both c^\dagger and c couple to the bath [36]. Since the coupling is energy dependent, each of c^\dagger and c gives a scaling factor $\sim \sqrt{T/T_{1\text{CK}}}$, leading to $1 - \mathcal{E}_F(|E_i\rangle) \sim |S_{z,ii}|^2 \sim (T/T_{1\text{CK}})^2$. In 2CK, S_z is rewritten as $S_z = i\gamma_+ \gamma_-$. Here, only a Majorana fermion γ_- , a “half” of $c^{(\dagger)}$, couples to the bath, providing the factor $\sim \sqrt{T/T_{2\text{CK}}}$; the other Majorana γ_+ is decoupled, not giving T independence. This causes the exponent halving in 2CK. It is non-Fermi liquid behavior.

The dependence of \mathcal{E}_F on L is obtained for 1CK in Fig. 2(c). $\mathcal{E}_F(L \rightarrow \infty) - \mathcal{E}_F(L)$ indicates entanglement

between $x > L$ and the rest. At $T = 0$, $\mathcal{E}_F = 1$ at $L \rightarrow \infty$ and decreases only slightly at $L > \xi_{1\text{CK}}$, implying that Kondo cloud lies mostly (more than 90 %) inside $\xi_{1\text{CK}}$. The cloud has a long tail of the power law at $L \gg \xi_{1\text{CK}}$,

$$\mathcal{E}_F \simeq 1 - b_1(\xi_{1\text{CK}}/L) \quad (1\text{CK}), \quad (5)$$

which is reproduced [37] with Yosida's ground state [39].

At finite T , the L dependence of \mathcal{E}_F characterizes the thermal reduction of Kondo cloud. We find that the cloud size, within which the majority of the cloud lies, is $\xi_{1\text{CK}}$ (almost insensitive to T) at $T \lesssim T_{1\text{CK}}$, and decreases with T at $T \gtrsim T_{1\text{CK}}$ [37]. Moreover, the two 1CK power laws in Eqs. (4) and (5) have different exponent, not connected by $L \leftrightarrow \hbar v_F/k_B T$ from the uncertainty principle, and they are additive at $L \gg \xi_{1\text{CK}}$ and $T \ll T_{1\text{CK}}$ as $1 - \mathcal{E}_F \simeq a_1(T/T_{1\text{CK}})^2 + b_1(\xi_{1\text{CK}}/L)$ [37]. These unusual results imply that entanglement suppression by thermal effects has different mechanism from that by the partial trace over $x > L$. The former reflects thermal entanglement suppression, while the latter measures the spatial extension of entanglement. Note that a mixed state obtained from a ground state by tracing out its subsystem is different from a thermal state, when the subsystem does not behave as a legitimate heat bath.

Finally, in contrast to EoF, correlations between the impurity spin and a conduction electron spin at L do not detect macroscopic entanglement, because of the entanglement monogamy [3] that tracing out all bath electrons except the one at L leaves only negligible entanglement. They measure the cloud tail differently from \mathcal{E}_F ; the spin-spin correlation [27] decays as $1/L^2$ at $L \gg \xi_{1\text{CK}}$, and the concurrence does not detect the cloud [40]. Impurity entanglement entropy [29, 30] detects macroscopic correlations, but it is not an entanglement measure; it decays as $\xi_{1\text{CK}}/L$ at $L \gg \xi_{1\text{CK}}$ as in Eq. (5), but as $T/T_{1\text{CK}}$ at

$T \ll T_{1\text{CK}}$, contrary to Eq. (4). Note that the cloud size at zero temperature was discussed in spin-chain Kondo models, using negativity [18, 19].

Perspective.— We have proposed a viable approach for computing macroscopic entanglement in thermal mixed states. Our study implies that EoF is a good tool for quantifying macroscopic quantumness in many-body mixed states; its original operational meaning [3] is a non-regularized entanglement cost in quantum information.

Our results indicate that the macroscopic entanglement characterizes the new aspects of many-body systems at finite temperature, inaccessible by conventional means and by EE. For example, it can identify the spatial extension of quantum correlations, the competition between the coexisting quantum and classical correlations induced by thermal effects or environments, and the fate of the zero-temperature correlations (e.g., topological order and quantum criticality) at finite temperature.

Our approach is optimized for computing entanglement between a few impurities and a macroscopic subsystem, and directly applicable to quantum impurity problems. It is in principle applicable to any convex-roof measures [13, 15], including multipartite entanglement [11, 12], and useful for experimental entanglement detection [13, 33]. It is desirable to extend our approach to study entanglement between macroscopic subsystems.

Experimental evidence of Kondo cloud remains elusive [24, 26]. It may be because the cloud is a macroscopic object entangled with an impurity, showing rapid quantum fluctuations with zero average spin. It will be valuable to find experimentally accessible EWs, to confirm the entanglement, hence, the cloud.

We thank Ehud Altman, Henrik Johannesson, and Jan von Delft for valuable discussions, Yong Hyun Kim for allowing us to use cluster computers in his group, and the support by Korea NRF (Grant No. 2013R1A2A2A01007327).

-
- [1] L. Amico, R. Fazio, A. Osterloh, and V. Vedral, *Rev. Mod. Phys.* **80**, 517 (2008).
 - [2] V. Vedral, *Nature* **453**, 1004 (2008).
 - [3] R. Horodecki, P. Horodecki, M. Horodecki, and K. Horodecki, *Rev. Mod. Phys.* **81**, 865 (2009).
 - [4] J. Eisert, M. Cramer, and M. B. Plenio, *Rev. Mod. Phys.* **82**, 277 (2010).
 - [5] A. Kitaev and J. Preskill, *Phys. Rev. Lett.* **96**, 110404 (2006).
 - [6] M. Levin and X.-G. Wen, *Phys. Rev. Lett.* **96**, 110405 (2006).
 - [7] G. Vidal, J. I. Latorre, E. Rico, and A. Kitaev, *Phys. Rev. Lett.* **90**, 227902 (2003).
 - [8] P. Calabrese and J. Cardy, *J. Phys. A: Math. Theor.* **42**, 504005 (2009).
 - [9] C. H. Bennett, D. P. DiVincenzo, J. A. Smolin, and W. K. Wootters, *Phys. Rev. A* **54**, 3824 (1996).
 - [10] B. Röthlisberger, J. Lehmann, and D. Loss, *Phys. Rev. A* **80**, 042301 (2009).
 - [11] S.-S. B. Lee and H.-S. Sim, *Phys. Rev. A* **85**, 022325 (2012).
 - [12] S. Ryu, S.-S. B. Lee, and H.-S. Sim, *Phys. Rev. A* **86**, 042324 (2012).
 - [13] O. Gühne and G. Tóth, *Phys. Rep.* **474**, 1 (2009).
 - [14] M. B. Plenio, *Science* **324**, 342 (2009).
 - [15] M. B. Plenio and S. Virmani, *Quant. Inf. Comp.* **7**, 1 (2007).
 - [16] G. Vidal and R. F. Werner, *Phys. Rev. A* **65**, 032314 (2002).
 - [17] M. B. Plenio, *Phys. Rev. Lett.* **95**, 090503 (2005).
 - [18] A. Bayat, P. Sodano, and S. Bose, *Phys. Rev. B* **81**, 064429 (2010).
 - [19] A. Bayat, S. Bose, P. Sodano, and H. Johannesson, *Phys. Rev. Lett.* **109**, 066403 (2012).
 - [20] P. Calabrese, J. Cardy, and E. Tonni, *Phys. Rev. Lett.* **109**, 130502 (2012).
 - [21] A. Ferraro, D. Cavalcanti, A. García-Saenz, and A. Acín, *Phys. Rev. Lett.* **100**, 080502 (2008).

- [22] R. A. Santos and V. E. Korepin, J. Phys. A: Math. Theor. **45**, 125307 (2012).
- [23] A. C. Hewson, *The Kondo Problems to Heavy Fermions* (Cambridge University Press, Cambridge, 1993).
- [24] I. Affleck, *Perspectives of Mesoscopic Physics* (World Scientific, 2010), pp. 1-44.
- [25] A. K. Mitchell, M. Becker, and R. Bulla, Phys. Rev. B **84**, 115120 (2011).
- [26] J. Park, S.-S. B. Lee, Y. Oreg, and H.-S. Sim, Phys. Rev. Lett. **110**, 246603 (2013).
- [27] L. Borda, Phys. Rev. B **75**, 041307(R) (2007).
- [28] A. Holzner, I. P. McCulloch, U. Schollwöck, J. von Delft, and F. Heidrich-Meisner, Phys. Rev. B **80**, 205114 (2009).
- [29] E. S. Sørensen, M.-S. Chang, N. Laflorencie, and I. Affleck, J. Stat. Mech. P08003 (2007).
- [30] E. Eriksson and H. Johannesson, Phys. Rev. B **84**, 041107(R) (2011).
- [31] F. G. S. L. Brandão, Phys. Rev. A **72**, 022310 (2005).
- [32] J. Eisert, F. G. S. L. Brandão, and K. M. R. Audenaert, New J. Phys. **9**, 46 (2007).
- [33] H. S. Park, S.-S. B. Lee, H. Kim, S.-K. Choi, and H.-S. Sim, Phys. Rev. Lett. **105**, 230404 (2010).
- [34] A. Weichselbaum and J. von Delft, Phys. Rev. Lett. **99**, 076402 (2007).
- [35] R. Bulla, T. A. Costi, and T. Pruschke, Rev. Mod. Phys. **80**, 395 (2008).
- [36] G. Zaránd and J. von Delft, Phys. Rev. B **61**, 6918 (2000).
- [37] See Supplemental Material for the details of our approach and some supplementary results. It includes Ref. [38].
- [38] W. K. Wootters, Phys. Rev. Lett. **80**, 2245 (1998).
- [39] K. Yosida, Phys. Rev. **147**, 223 (1966).
- [40] S. Oh and J. Kim, Phys. Rev. B **73**, 052407 (2006).

Supplementary Material for “Macroscopic quantum entanglement of Kondo cloud at finite temperature”

Here we provide the details of our approaches and some supplementary results. In Sec. I, we briefly introduce the Kondo models. In Sec. II, we describe how to numerically construct the thermal mixed states of the Kondo models by NRG, and give the NRG parameters. In Sec. III, we describe in details the way of tracing out the subsystem in $x > L$, within the NRG formalism. In Sec. IV, we derive the “two-qubit” EW $X_{2\text{qb}}$. In Sec. V, we prove that the sum $X = \sum_i X_i$ is a valid EW, and discuss how to choose the bath basis $\{|\phi_{i\eta}\rangle\}_{i\eta}$. In Sec. VI, we give the way to obtain the upper bound of $\mathcal{E}_F(\rho)$. In Sec. VII, we analyze the scaling behavior of the thermal suppression of \mathcal{E}_F in Eq. (4) in the main text, using the finite-size bosonization method. In Sec. VIII, we reproduce the long-tail scaling of $\mathcal{E}_F(L)$ in Eq. (5) in the main text, using the Yosida’s variational ground state. In Sec. IX, we give the computation result of EoF for 1CK when both T and L are finite, to discuss the size of the Kondo cloud at finite T . We also address that, at $T \ll T_{1\text{CK}}$ and $L \gg \xi_{1\text{CK}}$, two power-law decays are additive.

I. KONDO HAMILTONIAN

In 1CK (2CK), a spin-1/2 impurity is antiferromagnetically coupled with the spin(s) of a single channel (two channels) of the conduction electron bath at the impurity site [23]. Without loss of generality, we consider a semi-infinite one-dimensional bath ranging from $x = 0$ (the impurity site) to $x \rightarrow \infty$. Its Hamiltonian is

$$H = J \sum_{\alpha} \vec{S} \cdot \vec{s}_{\alpha} + \sum_{\alpha k \sigma} \epsilon_k c_{\alpha k \sigma}^{\dagger} c_{\alpha k \sigma}, \quad (\text{S1})$$

where J is the coupling strength, \vec{S} is the impurity spin operator, $\vec{s}_{\alpha} = \sum_{k k' \sigma \sigma'} c_{\alpha k \sigma}^{\dagger} \vec{\sigma}_{\sigma \sigma'} c_{\alpha k' \sigma'}/2$ is the electron spin operator in channel $\alpha \in [1, M]$ at the impurity site ($x = 0$), $M = 1$ (2) for 1CK (2CK), $\vec{\sigma}$ is Pauli matrix, $c_{\alpha k \sigma}^{\dagger}$ creates an electron with spin σ , momentum k , and energy $\epsilon_k = \hbar v_F(k - k_F) \in (-D, D)$ in α , constant density of states $\nu = 1/2D$, k_F is Fermi momentum, and D is the bandwidth. In this work, we consider the following case: The two channels of 2CK have the same coupling strength, and there is no external magnetic field. We use 1CK Kondo temperature $k_B T_{1\text{CK}} = D\sqrt{\nu J}e^{-1/\nu J}$, and determine $T_{2\text{CK}}$ from energy-eigenvalue convergence in NRG.

II. DENSITY MATRIX BY NRG

In NRG [35], each channel is logarithmically discretized and mapped onto a tight-binding chain (so-called Wilson chain) of length N , whose Hamiltonian is $H_N = J\vec{S} \cdot \sum_{\alpha \sigma \sigma'} f_{\alpha 0 \sigma}^{\dagger} \frac{\vec{\sigma}_{\sigma \sigma'}}{2} f_{\alpha 0 \sigma'} + \sum_{n=0}^N \sum_{\alpha \sigma} (t_n f_{\alpha n \sigma}^{\dagger} f_{\alpha n+1 \sigma} + \text{H.c.})$, where $f_{\alpha n \sigma}^{\dagger}$ creates an electron in the single-particle state $|\alpha n \sigma\rangle$ of spin σ in channel α at site n , $t_n \sim D\Lambda^{-n/2}$, and Λ is the discretization parameter. $|\alpha n \sigma\rangle$ has energy $\sim D\Lambda^{-n/2}$ and extends over length $\sim k_F^{-1}\Lambda^{n/2}$. H_N is iteratively diagonalized, based on the energy-scale hierarchy. At each (n -th) iteration step, only the lowest-lying energy eigenstates $\{|E_{ni}^K\rangle\}_i$ of the Hamiltonian of the step are kept to construct the next-step Hamiltonian, while the rest $\{|E_{ni}^D\rangle\}_i$ is discarded. The discarded states are the energy eigenstates of H_N , $H_N|E_{ni}^D\rangle \otimes \bigotimes_{\alpha; n' > n} |s_{\alpha n'}\rangle \approx E_{ni}^D|E_{ni}^D\rangle \otimes \bigotimes_{\alpha; n' > n} |s_{\alpha n'}\rangle$, where $|s_{\alpha n}\rangle = 0, \uparrow, \downarrow, \uparrow\downarrow$ denote the occupation basis states of site n and channel α .

The equilibrium state at temperature T is constructed [34] as

$$\rho(T) = \sum_n \rho_n \otimes I_{>n}, \quad \rho_n = \sum_i \frac{e^{-E_{ni}^D/k_B T}}{Z} |E_{ni}^D\rangle \langle E_{ni}^D|, \quad I_{>n} = \bigotimes_{\alpha; n' > n} \sum_s |s_{\alpha n'}\rangle \langle s_{\alpha n'}|, \quad (\text{S2})$$

where k_B is Boltzmann constant and Z is the partition function. Each block ρ_n covers energy $\sim D\Lambda^{-n/2}$ and length $\sim k_F^{-1}\Lambda^{n/2}$. $\text{Tr}(\rho_n \otimes I_{>n})$ is maximal near $n = n_T \equiv -2\log_{\Lambda}(k_B T/D)$ due to the competition between Boltzmann factor $e^{-D\Lambda^{-n/2}/k_B T}$ and degeneracy $\text{Tr} I_{>n} = 4^{N-n}$. In this work, we choose $\Lambda = 4$, $J/D = 0.3$, and the number of kept states $\lesssim 300$ at each iteration, and use the z -averaging [35] with $z = 0$ and 0.5 .

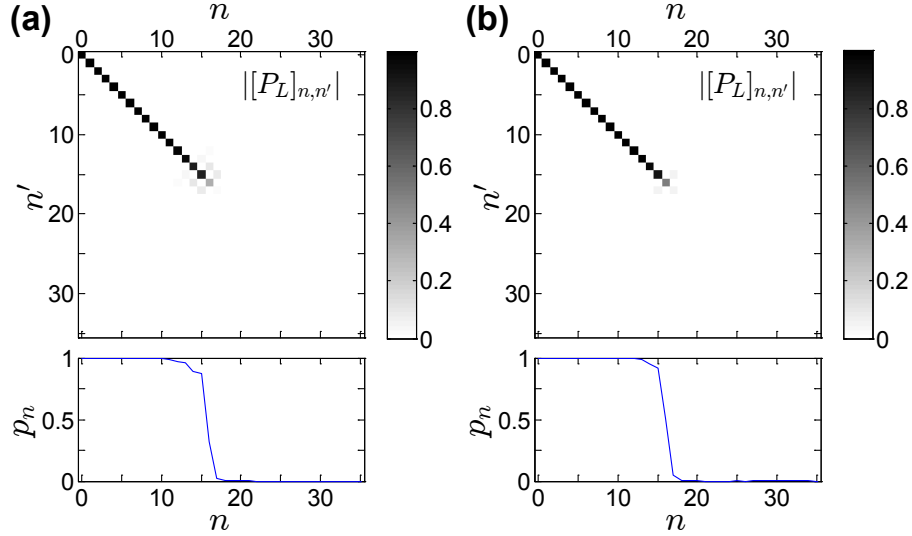


FIG. S1. $|[P_L]_{nn'}|$ (upper panels) and $p_n \equiv [P_L]_{nn}$ (lower panels) for (a) $\Lambda = 4$ and (b) $\Lambda = 8$. L is chosen to be Λ dependent as $L = k_F^{-1}\Lambda^8$ for comparison; $n_L = 16$ for both of (a) and (b). Note that for $\Lambda = 4$, the largest off-diagonal element of $[P_L]_{nn'}$ is ~ 0.07 and the other off-diagonal ones are smaller by one or more orders. We choose $z = 0$.

III. PARTIAL TRACE OVER $x > L$

We develop a way of obtaining, from NRG state $\rho(T)$, the reduced density matrix $\rho(T, L)$ of the impurity and electrons in $x \leq L$, by tracing out states in $x > L$. We use the projector to $x \leq L$,

$$P_L = \frac{1}{a} \int_0^L dx |x\rangle\langle x|. \quad (\text{S3})$$

$|x\rangle$ is the state spatially localized at x and a is lattice constant. One has $\langle \alpha n \sigma | P_L | \alpha' n' \sigma' \rangle = \delta_{\alpha\alpha'} \delta_{\sigma\sigma'} [P_L]_{nn'}$. The matrix $[P_L]_{nn'}$ is real symmetric and almost diagonal (see Fig. S1). Its diagonal part $[P_L]_{nn}$ is finite for $n \lesssim n_L \equiv 2 \log_\Lambda k_F L$, and vanishes for $n \gtrsim n_L$, reflecting the length scales of NRG sites. Off-diagonal parts $[P_L]_{nn'}$ are much smaller than diagonal ones, and decrease with increasing Λ , since spatial separation between $|\alpha n \sigma\rangle$'s increases. Based on this observation, we neglect the off-diagonal elements. The insensitivity of our computation of $\mathcal{E}_F(\rho)$ to Λ implies that this is a good approximation.

Neglecting the off-diagonal parts of $[P_L]_{nn'}$, we decompose $|\alpha n \sigma\rangle$ into the states of $x \leq L$ and $x > L$ as $f_{\alpha n \sigma}^\dagger = \sqrt{p_n} f_{\alpha n \sigma, \text{in}}^\dagger + \sqrt{1 - p_n} f_{\alpha n \sigma, \text{out}}^\dagger$ where $p_n \equiv [P_L]_{nn}$. Then the many-body occupation basis state $|s_{\alpha n}\rangle$ of site n and channel α is expressed as

$$\begin{aligned} |0_{\alpha n}\rangle &= |0_{\alpha n}^{\text{out}}\rangle |0_{\alpha n}^{\text{in}}\rangle, \\ |\uparrow_{\alpha n}\rangle &= f_{\alpha n \uparrow}^\dagger |0_{\alpha n}\rangle \\ &= (\sqrt{p_n} f_{\alpha n \uparrow, \text{in}}^\dagger + \sqrt{1 - p_n} f_{\alpha n \uparrow, \text{out}}^\dagger) |0_{\alpha n}^{\text{out}}\rangle |0_{\alpha n}^{\text{in}}\rangle \\ &= \sqrt{p_n} |0_{\alpha n}^{\text{out}}\rangle |\uparrow_{\alpha n}^{\text{in}}\rangle + \sqrt{1 - p_n} |\uparrow_{\alpha n}^{\text{out}}\rangle |0_{\alpha n}^{\text{in}}\rangle, \\ |\downarrow_{\alpha n}\rangle &= f_{\alpha n \downarrow}^\dagger |0_{\alpha n}\rangle \\ &= (\sqrt{p_n} f_{\alpha n \downarrow, \text{in}}^\dagger + \sqrt{1 - p_n} f_{\alpha n \downarrow, \text{out}}^\dagger) |0_{\alpha n}^{\text{out}}\rangle |0_{\alpha n}^{\text{in}}\rangle \\ &= \sqrt{p_n} |0_{\alpha n}^{\text{out}}\rangle |\downarrow_{\alpha n}^{\text{in}}\rangle + \sqrt{1 - p_n} |\downarrow_{\alpha n}^{\text{out}}\rangle |0_{\alpha n}^{\text{in}}\rangle, \\ |\uparrow\downarrow_{\alpha n}\rangle &= f_{\alpha n \uparrow}^\dagger f_{\alpha n \downarrow}^\dagger |0_{\alpha n}\rangle \\ &= p_n |0_{\alpha n}^{\text{out}}\rangle |\uparrow\downarrow_{\alpha n}^{\text{in}}\rangle + \sqrt{p_n(1 - p_n)} |\uparrow_{\alpha n}^{\text{out}}\rangle |\downarrow_{\alpha n}^{\text{in}}\rangle - \sqrt{p_n(1 - p_n)} |\downarrow_{\alpha n}^{\text{out}}\rangle |\uparrow_{\alpha n}^{\text{in}}\rangle + (1 - p_n) |\uparrow\downarrow_{\alpha n}^{\text{out}}\rangle |0_{\alpha n}^{\text{in}}\rangle. \end{aligned}$$

where $|s_{\alpha n}^{\text{in(out)}}\rangle$ describes the occupation $s = 0, \uparrow, \downarrow, \uparrow\downarrow$ in the $x \leq L$ ($x > L$) part of site n and channel α . The Hilbert space of $x \leq L$ ($x > L$) is spanned by $\bigotimes_{\alpha; n} \{|s_{\alpha n}^{\text{in(out)}}\rangle\}_s$. In this representation, tracing out $x > L$ is equivalent to

partial trace over $\bigotimes_{\alpha;n} \{|s_{\alpha n}^{\text{out}}\rangle\}_s$.

The partial trace over $\bigotimes_{\alpha;n} \{|s_{\alpha n}^{\text{out}}\rangle\}_s$ can be efficiently done for $\rho(T)$ in Eq. (S2) as $\rho(T, L) = \text{Tr}_0^{\text{out}} \cdots \text{Tr}_N^{\text{out}} \rho(T)$, where $\text{Tr}_n^{\text{out}}(\cdot) \equiv \text{Tr}_{\alpha=1,n}^{\text{out}} \cdots \text{Tr}_{\alpha=M,n}^{\text{out}}(\cdot)$ is the partial trace applied to site n and $\text{Tr}_{\alpha n}^{\text{out}}(\cdot) \equiv \sum_s \langle s_{\alpha n}^{\text{out}} | \cdot | s_{\alpha n}^{\text{out}} \rangle$. By choosing appropriate basis states $|r_{ni}\rangle \in \text{span} \bigotimes_{\alpha;n' \leq n} \{|s_{\alpha n'}^{\text{in}}\rangle\}_s$, we express $\rho(T, L)$, the result of the partial trace, as the block diagonal form of

$$\rho(T, L) = \sum_n \rho_n^{\text{in}} \otimes I_{>n}^{\text{in}}, \quad \rho_n^{\text{in}} = \sum_i r_{ni} |r_{ni}\rangle \langle r_{ni}|, \quad I_{>n}^{\text{in}} = \bigotimes_{\alpha;n' > n} \sum_s |s_{\alpha n'}^{\text{in}}\rangle \langle s_{\alpha n'}^{\text{in}}|.$$

This form corresponds to Eq. (S2) with $\rho_n \rightarrow \rho_n^{\text{in}}$, $I_{>n} \rightarrow I_{>n}^{\text{in}}$, and $|E_{ni}^{\text{D}}\rangle \otimes \bigotimes_{\alpha;n' > n} |s_{\alpha n'}\rangle \rightarrow |r_{ni}\rangle \otimes \bigotimes_{\alpha;n' > n} |s_{\alpha n'}^{\text{in}}\rangle$. $\text{Tr}(\rho_n^{\text{in}} \otimes I_{>n}^{\text{in}})$ is maximal near $n = \min\{n_T, n_L\}$. As ρ_n 's are defined not spatially but energetically, ρ_n^{in} can be contributed from many ρ_n 's. In this form, we generalize the concept of the kept and discarded states used for $\rho(T)$ into $\rho(T, L)$. In each step of constructing ρ_n^{in} , $|r_{ni}\rangle$'s are the “discarded” states with small r_{ni} , while there are the “kept” states used for constructing $\rho_{n' > n}^{\text{in}}$. This form is useful for reducing the total number of basis states ($|r_{ni}\rangle$'s), hence, computation cost. It is similar to the truncation of density matrix renormalization group methods, and allows us to handle $\rho(T, L)$ with similar cost of computing $\rho(T)$.

IV. DERIVATION OF TWO-QUBIT EW

We derive the optimal witness operator $X_{2\text{qb}}$ for the EoF $\mathcal{E}_F(\rho_{2\text{qb}})$ of an arbitrary (unnormalized) two-qubit state $\rho_{2\text{qb}}$ in the Hilbert space $\mathcal{H}_{2\text{qb}} = \{|0\rangle, |1\rangle\} \otimes \{|0\rangle, |1\rangle\}$. The derivation consists of two steps: (i) Construct the EW $X_{2\text{qb}}^{\mathcal{C}}$ [33] for the concurrence [38] $\mathcal{C}(\rho_{2\text{qb}})$, and (ii) deduce $X_{2\text{qb}}$ from $X_{2\text{qb}}^{\mathcal{C}}$ by using the relation between the EoF and the concurrence; for any normalized two-qubit state $\rho_{2\text{qb}}/\text{Tr}\rho_{2\text{qb}}$, \mathcal{E}_F satisfies $\mathcal{E}_F(\rho_{2\text{qb}}/\text{Tr}\rho_{2\text{qb}}) = f(\mathcal{C}(\rho_{2\text{qb}}/\text{Tr}\rho_{2\text{qb}}))$. Here, $f(x) = h((1 + \sqrt{1-x^2})/2)$ and $h(x) = -x \log_2 x - (1-x) \log_2 (1-x)$. Note that $\mathcal{E}_F(\rho_{2\text{qb}}/\text{Tr}\rho_{2\text{qb}}) = \mathcal{E}_F(\rho_{2\text{qb}})/\text{Tr}\rho_{2\text{qb}}$ and $\mathcal{C}(\rho_{2\text{qb}}/\text{Tr}\rho_{2\text{qb}}) = \mathcal{C}(\rho_{2\text{qb}})/\text{Tr}\rho_{2\text{qb}}$; this type of relations holds for all convex-roof entanglement measures and beyond two qubits [11] and it is consistent with Eq. (2). This is useful, as the “two-qubit” state $\rho_i = I_i \rho I_i$ in the main text is usually unnormalized.

The derivation of $X_{2\text{qb}}$ starts with the optimal witness operator $X_{2\text{qb}}^{\mathcal{C}}$ for $\mathcal{C}(\rho_{2\text{qb}})$. In the case of $\mathcal{C}(\rho_{2\text{qb}}) \neq 0$, it is obtained [11, 33] as

$$\mathcal{C}(\rho_{2\text{qb}}) = \text{Tr} X_{2\text{qb}}^{\mathcal{C}} \rho_{2\text{qb}} = \sup_{\mathcal{O}} \text{Tr} [\mathcal{O} (2|\Psi\rangle\langle\Psi| - I_{2\text{qb}}) \mathcal{O}^\dagger \rho_{2\text{qb}}], \quad \mathcal{O} = \mathcal{O}_1 \otimes \mathcal{O}_2, \quad (\text{S4})$$

where \mathcal{O}_i are local operators with determinant 1, each acting on $\{|0\rangle, |1\rangle\}$. Here $|\Psi\rangle = (|0\rangle|0\rangle + |1\rangle|1\rangle)/\sqrt{2}$ is maximally entangled ($\mathcal{E}_F = 1$) Bell state. In Eq. (S4), $X_{2\text{qb}}^{\mathcal{C}}$ is found by searching the optimal SLOCC (stochastic local quantum operations and classical communications in quantum information theory) operator \mathcal{O} on $\mathcal{H}_{2\text{qb}}$ that makes $\text{Tr} [\mathcal{O} (2|\Psi\rangle\langle\Psi| - I_{2\text{qb}}) \mathcal{O}^\dagger \rho_{2\text{qb}}]$ the largest. The form of Eq. (S4) captures the invariance of \mathcal{C} under SLOCC. In the case of $\mathcal{C}(\rho_{2\text{qb}}) = 0$, on the other hand, we choose $X_{2\text{qb}}^{\mathcal{C}} = 0$ (the null operator). $X_{2\text{qb}}^{\mathcal{C}}$ provides $\mathcal{C}(\rho_{2\text{qb}}) = \text{Tr} X_{2\text{qb}}^{\mathcal{C}} \rho_{2\text{qb}}$. Searching the optimal operator \mathcal{O} can be easily done by the singular value decomposition of the local operators as $\mathcal{O}_i = U_{1i} F_i U_{2i}$, where U 's are 2×2 local unitary operators and F is a local filtering operator [33]; in the matrix representation, F is written as $\begin{pmatrix} f & 0 \\ 0 & 1/f \end{pmatrix}$ with real f .

$X_{2\text{qb}}$ is obtained from $X_{2\text{qb}}^{\mathcal{C}}$ and $\mathcal{E}_F(\rho_{2\text{qb}}/\text{Tr}\rho_{2\text{qb}}) = f(\mathcal{C}(\rho_{2\text{qb}}/\text{Tr}\rho_{2\text{qb}}))$. As $f(x)$ is monotonically increasing and convex, one has $f(x) \geq f(x_\rho) + \frac{df}{dx}\big|_{x=x_\rho} (x - x_\rho)$ at any x_ρ and x . Substituting $x_\rho = \mathcal{C}(\rho_{2\text{qb}}/\text{Tr}\rho_{2\text{qb}})$, $f(x) \rightarrow X_{2\text{qb}}$, $x \rightarrow X_{2\text{qb}}^{\mathcal{C}}$, and $1 \rightarrow I_{2\text{qb}}$, we choose

$$X_{2\text{qb}} = f(x_\rho) I_{2\text{qb}} + \frac{df}{dx}\bigg|_{x=x_\rho} (X_{2\text{qb}}^{\mathcal{C}} - x_\rho I_{2\text{qb}}), \quad x_\rho = \mathcal{C}(\rho_{2\text{qb}}/\text{Tr}\rho_{2\text{qb}}) = \mathcal{C}(\rho_{2\text{qb}})/\text{Tr}\rho_{2\text{qb}}. \quad (\text{S5})$$

This operator $X_{2\text{qb}}$ is a witness operator for \mathcal{E}_F , since for any state $\rho' \in \mathcal{H}_{2\text{qb}}$, $\text{Tr} X_{2\text{qb}} \rho' \leq \mathcal{E}_F(\rho')$; one can check $\text{Tr} X_{2\text{qb}} \rho' \leq f(x_\rho) \text{Tr} \rho' + \frac{df}{dx}\big|_{x=x_\rho} (\mathcal{C}(\rho') - x_\rho \text{Tr} \rho') \leq f(\mathcal{C}(\rho'/\text{Tr}\rho')) \text{Tr} \rho' = \mathcal{E}_F(\rho'/\text{Tr}\rho') \text{Tr} \rho' = \mathcal{E}_F(\rho')$, using the convexity of $f(x)$ and Eq. (2). Moreover, it is easy to show that $X_{2\text{qb}}$ satisfies $\text{Tr}(X_{2\text{qb}} \rho_{2\text{qb}}) = \mathcal{E}_F(\rho_{2\text{qb}})$, using $\text{Tr}(X_{2\text{qb}}^{\mathcal{C}} \rho_{2\text{qb}}) = \mathcal{C}(\rho_{2\text{qb}})$. Therefore $X_{2\text{qb}}$ is the optimal witness operator for $\mathcal{E}_F(\rho_{2\text{qb}})$. Note that the elements of $\mathbb{P}_{X_{2\text{qb}}} = \{|\psi\rangle | \mathcal{E}_F(|\psi\rangle) = \langle\psi| X_{2\text{qb}} |\psi\rangle = \mathcal{E}_F(\rho_{2\text{qb}})\}$ constitute the optimal pure-state decomposition for $\mathcal{E}_F(\rho_{2\text{qb}})$ [38].

V. WITNESS OPERATOR $X = \sum_i X_i$

In the main text, we divide the whole Hilbert space \mathcal{H} into “two-qubit” subspaces $\mathcal{H}_i \equiv \text{span}\{|\eta\rangle \otimes |\phi_{i\eta'}\rangle\}_{\eta\eta'}$ and obtain the optimal witness operator X_i for $\mathcal{E}_F(\rho_i)$, directly from X_i ; $\rho_i = I_i \rho I_i$ is the projection of ρ to \mathcal{H}_i and $\text{Tr} X_i \rho_i = \mathcal{E}_F(\rho_i)$. We here (i) prove that $X = \sum_i X_i$ is a witness operator for $\mathcal{E}_F(\rho)$, namely that $\text{Tr} X \rho$ is a lower bound of $\mathcal{E}_F(\rho)$, and also (ii) discuss a strategy how to optimize X_i ’s.

The task (i) is equivalent, according to Eq. (2), to proving that $\text{Tr}(X|\psi\rangle\langle\psi|) \leq \mathcal{E}_F(|\psi\rangle)$ for any normalized pure state $|\psi\rangle$ in \mathcal{H} . To prove it, we decompose $|\psi\rangle = \sum_i |\psi_i\rangle$, where $|\psi_i\rangle$ is the projection of $|\psi\rangle$ onto \mathcal{H}_i . Applying Schmidt decomposition to $|\psi_i\rangle$, $|\psi_i\rangle = c_{\uparrow i} |\uparrow\rangle |\phi'_{i\uparrow}\rangle + c_{\downarrow i} |\downarrow\rangle |\phi'_{i\downarrow}\rangle$ and $\langle\phi'_{i\eta}|\phi'_{i'\eta'}\rangle = \delta_{ii'} \delta_{\eta\eta'}$, one has $\mathcal{E}_F(|\psi\rangle) = h(\sum_i |c_{\uparrow i}|^2) = h(\sum_i |c_{\downarrow i}|^2)$ where $h(x) = -x \log_2 x - (1-x) \log_2 (1-x)$. It satisfies $\mathcal{E}_F(|\psi\rangle) \geq \sum_i \mathcal{E}_F(|\psi_i\rangle) \geq \sum_i \langle\psi_i|X_i|\psi_i\rangle = \text{Tr}(\sum_i X_i |\psi\rangle\langle\psi|)$; the first inequality is from the concavity of $h(x)$, $h(\sum_i |c_{\uparrow i}|^2) \geq \sum_i (|c_{\uparrow i}|^2 + |c_{\downarrow i}|^2) h(\frac{|c_{\uparrow i}|^2}{|c_{\uparrow i}|^2 + |c_{\downarrow i}|^2})$, and also from $\mathcal{E}_F(|\psi_i\rangle) = \langle\psi_i|\mathcal{E}_F(|\psi_i\rangle/\sqrt{\langle\psi_i|\psi_i\rangle})$, and the second from the fact that X_i is a witness operator for the EoF of two-qubit states (which was proved above). This proves that X is a witness operator for $\mathcal{E}_F(\rho)$.

Next, we discuss a strategy how to find $X = \sum_i X_i$ that provides a better lower bound of $\mathcal{E}_F(\rho)$. One needs to first decompose \mathcal{H} into \mathcal{H}_i ’s. Among many possible ways for it, we choose a NRG-based way. In this way, we decompose ρ into “units”, and choose the basis state set $\text{span}\{|\eta\rangle \otimes |\phi_{i\eta'}\rangle\}_{i\eta\eta'}$ of each unit. Each unit has one or a few successive NRG diagonal blocks of ρ , and different units have no overlap; the number of blocks in a unit is chosen to have a better lower bound of $\mathcal{E}_F(\rho)$. Then $\{|\uparrow\rangle, |\downarrow\rangle\} \otimes \{|\phi_{i\uparrow}\rangle, |\phi_{i\downarrow}\rangle\}$ constitutes \mathcal{H}_i . This way is naturally expected to lead to a good lower bound, as the NRG blocks capture the main physics. After choosing \mathcal{H}_i ’s, we find the optimal witness X_i (equivalently X_i^c) for $\mathcal{E}_F(\rho_i) = \text{Tr} X_i \rho_i$, following Eqs. (S4) and (S5). We skip other technical details of finding X , such as how to choose the basis states $\{|\phi_{i\eta}\rangle\}_{i\eta}$.

VI. UPPER BOUND OF $\mathcal{E}_F(\rho)$

In the above, we find $X = \sum_i X_i$ that provides the best lower bound of $\mathcal{E}_F(\rho)$ within the form utilizing Eq. (S5). We call this operator as X_ρ^{opt} . A good upper bound is also obtained from X_ρ^{opt} , by finding a set of pure states $\mathbb{P}_{X_\rho^{\text{opt}}} = \{|\psi\rangle | \langle\psi|X_\rho^{\text{opt}}|\psi\rangle = \mathcal{E}_F(|\psi\rangle)\}$ and a decomposition $\rho = \sum_l p_l' |\psi_l'\rangle\langle\psi_l'|$ where each $|\psi_l'\rangle$ is sufficiently similar to an element of $\mathbb{P}_{X_\rho^{\text{opt}}}$. We suggest below a systematic way of finding the decomposition $\rho = \sum_l p_l' |\psi_l'\rangle\langle\psi_l'|$.

To find the decomposition, we diagonalize $\rho = \sum_d \bar{p}_d |\bar{\psi}_d\rangle\langle\bar{\psi}_d|$, where $\langle\bar{\psi}_d|\bar{\psi}_{d'}\rangle = \delta_{dd'}$. Any pure-state decomposition $\rho = \sum_l q_l |\varphi_l\rangle\langle\varphi_l|$ is generated by a left-unitary matrix U as $\sqrt{q_l} |\varphi_l\rangle = \sum_d U_{ld} \sqrt{\bar{p}_d} |\bar{\psi}_d\rangle$ and $U^\dagger U = I$. To generate $\{|\varphi_l\rangle\}$ close to $\mathbb{P}_{X_\rho^{\text{opt}}} = \{|\psi_l\rangle\}$, we introduce a matrix W , $[W]_{ld} = \langle\bar{\psi}_d|\psi_l\rangle p_l^{y_1} \bar{p}_d^{y_2}$, and obtain its singular value decomposition of $W = V_L \Sigma V_R^\dagger$, where y_1 and y_2 are the variables to be optimized. Here, p_l ’s are chosen to satisfy $\rho \simeq \sum_l p_l |\psi_l\rangle\langle\psi_l|$. Then, we choose U as $U = V_L V_R^\dagger$, and use it to obtain $\{|\psi_l'\rangle\}$ via $\sqrt{p_l'} |\psi_l'\rangle = \sum_d U_{ld} \sqrt{\bar{p}_d} |\bar{\psi}_d\rangle$. Finally, we optimize y_1 and y_2 to minimize $\sum_l p_l' \mathcal{E}_F(|\psi_l'\rangle)$. The minimum value of $\sum_l p_l' \mathcal{E}_F(|\psi_l'\rangle)$ is a good upper bound of $\mathcal{E}_F(\rho)$.

In the above way of finding an upper bound, it takes heavy numerical cost to handle ρ as a whole, since ρ has a large size. To avoid the heavy cost, we decompose $\rho = \sum_n \rho_n$ into the NRG blocks ρ_n ’s (or the units of a few successive blocks), construct a witness operator X_n for $\mathcal{E}_F(\rho_n)$, and find a good upper bound \mathcal{E}_n of $\mathcal{E}_F(\rho_n)$, using \mathbb{P}_{X_n} as mentioned above. The sum $\sum_n \mathcal{E}_n$ of the upper bound of $\mathcal{E}_F(\rho_n)$ over n ’s provides a good upper bound of $\mathcal{E}_F(\rho)$. Note that $\sum_n X_n$ is not necessarily a witness operator of ρ ; it is because X_n is not necessarily constructed by the bath states orthogonal between different NRG blocks (or units), contrary to $X = \sum_i X_i$.

VII. T DEPENDENCE OF \mathcal{E}_F FROM BOSONIZATION

We here confirm the universal power-law thermal decay of \mathcal{E}_F , using finite-size bosonization and refermionization methods [36], and attribute the power-law exponents different between 1CK and 2CK to Majorana fermions emerging in 2CK.

For 1CK and 2CK, the thermal state has the form of $\rho = \sum_i w_i |E_i\rangle\langle E_i|$; w_i is Boltzmann weight. $|E_i\rangle = b_{i\uparrow} |\uparrow\rangle |e_{i\uparrow}\rangle + b_{i\downarrow} |\downarrow\rangle |e_{i\downarrow}\rangle$ is an energy eigenstate with energy E_i and an eigenstate of the total (impurity and bath) spin- z operator simultaneously. Bath states $|e_{i\eta}\rangle$ satisfy $\langle e_{i\uparrow} | e_{i\downarrow} \rangle = 0$ because $|e_{i\uparrow}\rangle$ and $|e_{i\downarrow}\rangle$ have different spin- z quantum numbers, while $\langle e_{i\eta} | e_{i'\neq i\eta} \rangle \neq 0$ in general. We focus on $|E_i\rangle$ ’s with $E_i \sim k_B T$, as they govern the properties of ρ ; this is due to the competition between degeneracy and Boltzmann weight. Using the bosonization, we will later show that for

$E_i, E_{i'} \sim k_B T \ll k_B T_{1\text{CK}, 2\text{CK}}$, $S_{z, ii'} \equiv \langle E_i | S_z | E_{i'} \rangle$ and $S_{-, ii'} \equiv \langle E_i | S_- | E_{i'} \rangle$ satisfy

$$S_{z, ii'}, S_{-, ii'} \propto \begin{cases} T/T_{1\text{CK}}, & \text{for 1CK,} \\ \sqrt{T/T_{2\text{CK}}}, & \text{for 2CK.} \end{cases} \quad (\text{S6})$$

The S_z and S_- impurity spin operator, $S_z \equiv (|\uparrow\rangle\langle\uparrow| - |\downarrow\rangle\langle\downarrow|)/2$ and $S_- \equiv |\downarrow\rangle\langle\uparrow|$, have entanglement information. $S_{z, ii}$ connects with $\mathcal{E}_F(|E_i\rangle)$. $|E_i\rangle$ is maximally entangled when $S_{z, ii} = (|b_{i\uparrow}|^2 - |b_{i\downarrow}|^2)/2 = 0$, while it is separable when $S_{z, ii} = \pm 1/2$. We find that for $E_i/k_B \sim T \ll T_{1\text{CK}, 2\text{CK}}$, $|S_{z, ii}| \ll 1/2$ and $\mathcal{E}_F(|E_i\rangle) = h(\frac{1}{2} + S_{z, ii}) \simeq 1 - 2|S_{z, ii}|^2/\log 2$, where $h(x) = -x \log_2 x - (1-x) \log_2 (1-x)$. On the other hand, $S_{z, ii' \neq i}$ and $S_{-, ii' \neq i}$ have the information of state overlap $\langle e_{i\eta} | e_{i'\eta'} \rangle$. From Eq. (S6) and $\langle E_i | E_{i'} \rangle = \delta_{ii'}$, we find

$$\langle e_{i\eta} | e_{i'\eta'} \rangle - \delta_{ii'} \delta_{\eta\eta'} \propto \begin{cases} T/T_{1\text{CK}}, & \text{for 1CK,} \\ \sqrt{T/T_{2\text{CK}}}, & \text{for 2CK.} \end{cases} \quad (\text{S7})$$

The overlap results in entanglement reduction in a pure-state mixture, $\mathcal{E}_F(\sum_i w_i |E_i\rangle\langle E_i|) \leq \sum_i w_i \mathcal{E}_F(|E_i\rangle)$. From Eq. (1), $\mathcal{E}_{F,0} \equiv \sum_i w_i \mathcal{E}_F(|E_i\rangle) \simeq \sum_i w_i (1 - 2|S_{z, ii}|^2/\log 2)$ is an upper bound of $\mathcal{E}_F(\rho)$. The upper bound $\mathcal{E}_{F,0}$ and Eq. (S6) agree with the power law in Eq. (4).

We also confirm Eq. (4) using a lower bound of $\mathcal{E}_F(\rho)$. We consider a witness operator X' ,

$$X' = \sum_i \left[\frac{2}{\log 2} |\Psi_i\rangle\langle\Psi_i| - \left(\frac{2}{\log 2} - 1 \right) I_i \right], \quad (\text{S8})$$

$$|\Psi_i\rangle = \frac{1}{\sqrt{2}} (|\uparrow\rangle|\phi_{i\uparrow}\rangle + |\downarrow\rangle|\phi_{i\downarrow}\rangle), \quad I_i = \sum_{\eta=\uparrow, \downarrow; \eta'=\uparrow, \downarrow} |\eta\rangle\langle\eta| \otimes |\phi_{i\eta'}\rangle\langle\phi_{i\eta'}|.$$

This has the similar form to Eq. (3). Here, $|\phi_{i\eta}\rangle$'s are the orthonormal states obtained by applying the Gram-Schmidt orthonormalization process to the states $\{|e_{i\eta}\rangle\}$. Because $\langle e_{i\eta} | e_{i'\eta'} \rangle - \delta_{ii'} \delta_{\eta\eta'}$ is very small at $T \ll T_{1\text{CK}, 2\text{CK}}$ as in Eq. (S7), $|\phi_{i\eta}\rangle$ little deviates from $|e_{i\eta}\rangle$ as $b_{i\eta}|e_{i\eta}\rangle = (|\phi_{i\eta}\rangle + |\delta_{i\eta}\rangle)/\sqrt{2}$. The expectation value $\text{Tr} X' \rho$ is a lower bound of $\mathcal{E}_F(\rho)$. After some computation, we find

$$\text{Tr} X' \rho = 1 - \frac{1}{2 \log 2} \sum_{ii'} w_i [|\langle\phi_{i'\uparrow}|\delta_{i\uparrow}\rangle - \langle\phi_{i'\downarrow}|\delta_{i\downarrow}\rangle|^2 + 2(|\langle\phi_{i'\downarrow}|\delta_{i\uparrow}\rangle|^2 + |\langle\phi_{i'\uparrow}|\delta_{i\downarrow}\rangle|^2)].$$

Applying $|\delta_{i\eta}\rangle \propto T/T_{1\text{CK}}$ for 1CK and $|\delta_{i\eta}\rangle \propto \sqrt{T/T_{2\text{CK}}}$ for 2CK in Eq. (S7), we find that $\text{Tr} X' \rho$ satisfies Eq. (4). This analytic derivation of the same universal power-law behavior of the upper and lower bounds $\mathcal{E}_{F,0}$ and $\text{Tr} X' \rho$ strongly supports our numerical result of Eq. (4).

For a complete proof, we now derive Eq. (S6) and discuss the difference between 1CK and 2CK. We first consider 2CK. In 2CK, the electron bath has the four degrees of freedom, total charge, total spin, charge difference between the channels, and spin difference between the channels. According to the bosonization and refermionization along Emery-Kivelson line [36], the degree of freedom from the spin difference (decoupled from the others) is described by the resonant-level model, $H_x^{2\text{CK}} = \epsilon_d : c_d^\dagger c_d : + \sum_k \epsilon_k : c_k^\dagger c_k : + \sqrt{\Delta \Gamma} \sum_k (c_k^\dagger + c_k)(c_d - c_d^\dagger)$, where c_d^\dagger creates a pseudofermion in the resonant level coupled to a reservoir of pseudofermions (with momentum k and energy ϵ_k) created by c_k^\dagger , Δ is the level spacing of the reservoir, and $::$ means normal ordering. Γ is the broadening of the resonance and plays the role of Kondo temperature, $\Gamma = k_B T_{2\text{CK}}$. We choose Δ as $\Delta = k_B T$ to focus on energy scale $\sim k_B T$. c_d^\dagger (c_d) corresponds to impurity spin raising operator S_+ (lowering S_-), while $c_d^\dagger c_d = S_z + 1/2$. In our case of no external magnetic field, $\epsilon_d = 0$, and Majorana fermion $\gamma_{d+} = (c_d + c_d^\dagger)/\sqrt{2}$ decouples from $H_x^{2\text{CK}}$ (while the other Majorana $\gamma_{d-} = i(c_d^\dagger - c_d)/\sqrt{2}$ participates in $H_x^{2\text{CK}}$). Namely, a half of the impurity decouples from bath electrons, making 2CK a non-Fermi liquid. $H_x^{2\text{CK}}$ is diagonalized as $H_x^{2\text{CK}} = \sum_{\epsilon \geq 0} \epsilon c_{2\epsilon}^\dagger c_{2\epsilon} + \sum_{k > k_F} \epsilon_k d_k^\dagger d_k + (\text{const.})$. Meanwhile, each of other three degrees of freedom is bosonic and diagonalized as $\sum_q q b_{qy}^\dagger b_{qy}$, where b_{qy} is a bosonic operator for the degree of freedom y with momentum $q = n_q \Delta / \hbar v_F$ and n_q is a positive integer. The eigenstates $|\tilde{E}_i^{2\text{CK}}\rangle$ of the refermionized Hamiltonian are the direct products of the eigenstates of $H_x^{2\text{CK}}$ and the eigenstates of the three bosonic degrees of freedom.

We compute $S_{z, ii'} = \langle E_i^{2\text{CK}} | S_z | E_{i'}^{2\text{CK}} \rangle$. The eigenstates $|E_i^{2\text{CK}}\rangle$ of 2CK connects with the eigenstates $|\tilde{E}_i^{2\text{CK}}\rangle = U_{\text{EK}} |E_i^{2\text{CK}}\rangle$ via Emery-Kivelson transformation U_{EK} [36]. Since $U_{\text{EK}} S_z U_{\text{EK}}^\dagger = S_z = c_d^\dagger c_d - 1/2 = i\gamma_{d+}\gamma_{d-}$, $S_{z, ii'}$ is

written as $S_{z,ii'} = i\langle \tilde{E}_i^{2\text{CK}} | \gamma_{d+} \gamma_{d-} | \tilde{E}_{i'}^{2\text{CK}} \rangle$. After some calculations, we find

$$\begin{aligned} S_{z,ii'} &= i\langle \tilde{E}_i^{2\text{CK}} | \gamma_{d+} \gamma_{d-} | \tilde{E}_{i'}^{2\text{CK}} \rangle \\ &= \frac{1}{2} \sum_{\epsilon, \epsilon' \geq 0} B_{\epsilon d+} B_{\epsilon' d-} \langle \tilde{E}_i^{2\text{CK}} | (c_{2\epsilon} + c_{2\epsilon}^\dagger)(c_{2\epsilon'}^\dagger - c_{2\epsilon'}) | \tilde{E}_{i'}^{2\text{CK}} \rangle \\ &= \frac{1}{2} \sum_{\epsilon' \geq 0} B_{\epsilon' d-} \langle \tilde{E}_i^{2\text{CK}} | (c_{2\epsilon=0}^\dagger + c_{2\epsilon=0})(c_{2\epsilon'}^\dagger - c_{2\epsilon'}) | \tilde{E}_{i'}^{2\text{CK}} \rangle, \end{aligned}$$

where coefficient $B_{\epsilon d\pm}$ connects $\gamma_{d\pm}$ and the excitation of $(c_{2\epsilon-}^\dagger \pm c_{2\epsilon-})/\sqrt{2}$ and $|\langle \tilde{E}_i^{2\text{CK}} | (c_{2\epsilon=0}^\dagger + c_{2\epsilon=0})(c_{2\epsilon'}^\dagger - c_{2\epsilon'}) | \tilde{E}_{i'}^{2\text{CK}} \rangle| = 1$ or 0 ; for the detail of $B_{\epsilon d\pm}$, see Ref. [36]. In the last equality, we used $B_{\epsilon d+} = \delta_{\epsilon 0}$, coming from the decoupling of Majorana fermion γ_{d+} from the bath. Since $B_{\epsilon d-} \propto \sqrt{T/T_{2\text{CK}}}$ at $T \ll T_{2\text{CK}}$, $S_{z,ii'} \propto \sqrt{T/T_{2\text{CK}}}$ in agreement with Eq. (S6).

We also compute $S_{-,ii'} = \langle E_i^{2\text{CK}} | S_- | E_{i'}^{2\text{CK}} \rangle$. Using U_{EK} and $c_d = F_s^\dagger S_-$, where F_s^\dagger is a Klein factor, we have $S_{-,ii'} = \langle \tilde{E}_i^{2\text{CK}} | e^{-i\varphi_s(0)} F_s c_d | \tilde{E}_{i'}^{2\text{CK}} \rangle$, where the boson field $\varphi_s(0)$ results from the commutation between S_- and U_{EK} ; see Ref. [36]. φ_s and F_s correspond to total charge degree of freedom. Here, F_s gives 1 or 0, hence, not related with $T/T_{2\text{CK}}$. And, $c_d = (c_{2\epsilon=0}^\dagger + c_{2\epsilon=0})/2 + O(\sqrt{T/T_{2\text{CK}}})$ does not provide $\sqrt{T/T_{2\text{CK}}}$ in the leading order term. In contrast, $e^{-i\varphi_s(0)}$ interestingly provides $e^{-i\varphi_s(0)} \propto \sqrt{T/T_{2\text{CK}}}$, since the bosonic reservoir, included in the resonant-level model as being decoupled from $H_x^{2\text{CK}}$, also has the finite length of $\sim \hbar v_F/\Delta \sim \hbar v_F/k_B T$. We show this, expanding $\varphi_s(0)$ in terms of boson operators b_{qs} , $\varphi_s(0) = \sum_{q>0} \frac{-1}{\sqrt{n_q}} (b_{qs}^\dagger + b_{qs}) e^{-aq/2}$, where $a \propto \Gamma^{-1}$ is the cutoff. Some calculations lead to

$$e^{-i\varphi_s(0)} = \prod_{q>0} \left[\exp \left(i \frac{1}{\sqrt{n_q}} b_{qs}^\dagger e^{-aq/2} \right) \exp \left(i \frac{1}{\sqrt{n_q}} b_{qs} e^{-aq/2} \right) \exp \left(-\frac{1}{2n_q} e^{-aq} \right) \right].$$

The first and second terms in the squared bracket are $O(1)$ since $|\tilde{E}_i^{2\text{CK}}\rangle$ are eigenstates of $b_{qs}^\dagger b_{qs}$ with eigenvalues 0 or 1. Meanwhile, $\prod_{q>0} \exp \left(-\frac{1}{2n_q} e^{-aq} \right) = \sqrt{1 - e^{-a\Delta/\hbar v_F}} \propto \sqrt{a\Delta} = \sqrt{T/T_{2\text{CK}}}$ at $T \ll T_{2\text{CK}}$. Hence, $S_{-,ii'} \propto \sqrt{T/T_{2\text{CK}}}$ is proved.

Next, we derive Eq. (S6) for 1CK. According to the bosonization and refermionization at Toulouse point [36], the spin degree of freedom of 1CK is also described by a similar resonant-level model, $H_s^{1\text{CK}} = \epsilon_d : c_d^\dagger c_d : + \sum_k \epsilon_k : c_k^\dagger c_k : + \sqrt{\Delta\Gamma} \sum_k (c_k^\dagger c_d + c_d^\dagger c_k) = \sum_\epsilon \epsilon : c_{1\epsilon}^\dagger c_{1\epsilon} : + (\text{const.})$, but with $\Gamma = k_B T_{1\text{CK}}$. Contrary to 2CK, it shows a Fermi liquid, and no Majorana fermion of the impurity decouples from the bath. We compute $S_{z,ii'} = \langle E_i^{1\text{CK}} | S_z | E_{i'}^{1\text{CK}} \rangle$, where $|\tilde{E}_i^{1\text{CK}}\rangle$'s denote the eigenstates of $H_s^{1\text{CK}}$. Using another Emery-Kivelson transformation $U_{\text{EK}}^{1\text{CK}}$, $|\tilde{E}_i^{1\text{CK}}\rangle = U_{\text{EK}}^{1\text{CK}} | E_i^{1\text{CK}} \rangle$, we find $S_{z,ii'} = \langle E_i^{1\text{CK}} | S_z | E_{i'}^{1\text{CK}} \rangle = \langle \tilde{E}_i^{1\text{CK}} | c_d^\dagger c_d | \tilde{E}_{i'}^{1\text{CK}} \rangle - \delta_{ii'}/2$, since $U_{\text{EK}}^{1\text{CK}} S_z (U_{\text{EK}}^{1\text{CK}})^\dagger = S_z = c_d^\dagger c_d - 1/2$. It is written as $S_{z,ii'} = \sum_{\epsilon\epsilon'} B_{\epsilon d} B_{\epsilon' d} \langle \tilde{E}_i^{1\text{CK}} | c_{1\epsilon}^\dagger c_{1\epsilon'} | \tilde{E}_{i'}^{1\text{CK}} \rangle - \delta_{ii'}/2$ in terms of the coefficients $B_{\epsilon d}$ connecting c_d and $c_{1\epsilon}$. Since $B_{\epsilon d} \propto \sqrt{T/T_{1\text{CK}}}$ at $T \ll T_{1\text{CK}}$ [36] and $\langle \tilde{E}_i^{1\text{CK}} | c_{1\epsilon}^\dagger c_{1\epsilon'} | \tilde{E}_{i'}^{1\text{CK}} \rangle = 1$ or 0 , we find $S_{z,ii' \neq i} \propto T/T_{1\text{CK}}$, in agreement with Eq. (S6). Similarly, it is straightforward to show $S_{z,ii} \propto T/T_{1\text{CK}}$.

We also compute $S_{-,ii'} = \langle E_i^{1\text{CK}} | S_- | E_{i'}^{1\text{CK}} \rangle$. The bosonization results in an expression similar to the 2CK, $S_{-,ii'} = \langle \tilde{E}_i^{1\text{CK}} | e^{-i(\sqrt{2}-1)\varphi_s(0)} e^{-i\pi S_z} c_d | \tilde{E}_{i'}^{1\text{CK}} \rangle$. It is however hard to handle $e^{-i(\sqrt{2}-1)\varphi_s(0)}$ with the irrational number $\sqrt{2}-1$ of Toulouse point. Instead, we study $S_{-,ii'}$ using an effective theory near the strong-coupling fixed point [23]. At the fixed point, the Kondo singlet state decouples from Fermi-liquid excitations. Near the fixed point at $T \ll T_{1\text{CK}}$, the singlet and the excitations are coupled, with coupling energy $\sim D\Lambda^{-(N-1)/4} \sim \sqrt{T}$. This modifies $|E_i^{1\text{CK}}\rangle$ from $|E_i^{1\text{CK},0}\rangle$ as $|E_i^{1\text{CK}}\rangle = |E_i^{1\text{CK},0}\rangle + |\delta_i\rangle$, where $|E_i^{1\text{CK},0}\rangle$'s are the states at the fixed point. The coupling energy leads to $\langle \delta_i | \delta_i \rangle \propto T$, resulting in $S_{-,ii'} \propto T$, in agreement with Eq. (S6). The same argument reproduces $S_{z,ii'} = \langle E_i^{1\text{CK}} | S_z | E_{i'}^{1\text{CK}} \rangle \propto T/T_{1\text{CK}}$, which was obtained using the bosonization in the above.

VIII. L DEPENDENCE OF \mathcal{E}_F FOR 1CK

Our numerical result of the L dependence of \mathcal{E}_F at $T = 0$ and $L \gg \xi_{1\text{CK}}$ in Eq. (5) is reproduced with the variational 1CK ground state by Yosida [39],

$$|\psi_Y\rangle = \frac{|\uparrow\uparrow\rangle|\phi_{Y\downarrow}\rangle - |\downarrow\downarrow\rangle|\phi_{Y\uparrow}\rangle}{\sqrt{2}}, \quad |\phi_{Y\sigma}\rangle = \phi_{Y\sigma}^\dagger |\text{FS}\rangle, \quad \phi_{Y\sigma}^\dagger = \frac{1}{\sqrt{N}} \sum_{k>k_F} \frac{c_{k\sigma}^\dagger}{\epsilon_k + E_Y},$$

where $|\text{FS}\rangle = \prod_{k \leq k_F; \sigma=\uparrow, \downarrow} c_{k\sigma}^\dagger |0\rangle$ is the Fermi sea of the bath, $|0\rangle$ is the vacuum state, \mathcal{N} is the normalization factor ensuring $|\langle \phi_{Y\sigma} | \phi_{Y\sigma} \rangle|^2 = 1$, and $E_Y = De^{-4/3 J\nu_F}$ corresponds to $k_B T_{1\text{CK}}$; we here use $c_{k\sigma}^\dagger \equiv c_{\alpha=1, k\sigma}^\dagger$. This illustrates the Kondo singlet of the impurity spin and the electron spin created by $\phi_{Y\sigma}^\dagger$. The spatial dependence of $\phi_{Y\sigma}^\dagger$ is $\phi_Y(x) = \frac{1}{\sqrt{N}} \sum_{k > k_F} \sqrt{\frac{2}{l}} \frac{\sin kx}{\epsilon_k + E_Y}$, where $l \rightarrow \infty$ is the total length of the one-dimensional bath and $E_Y \equiv \hbar v_F k_Y \simeq \hbar v_F / \xi_{1\text{CK}}$.

To study the L dependence of \mathcal{E}_F , we compute $\text{Tr}_{x>L} |\psi_Y\rangle \langle \psi_Y|$, by tracing out the states outside L . For this purpose, we decompose each single-electron operator,

$$c_{k\sigma}^\dagger = \sqrt{\frac{L}{l}} c_{k\sigma, \text{in}}^\dagger + \sqrt{1 - \frac{L}{l}} c_{k\sigma, \text{out}}^\dagger, \quad \phi_{Y\sigma}^\dagger = \sqrt{1-p} \phi_{Y\sigma, \text{in}}^\dagger + \sqrt{p} \phi_{Y\sigma, \text{out}}^\dagger,$$

where $c_{k\sigma, \text{in(out)}}^\dagger \sim \int_{x \leq L(x>L)} dx c_{x\sigma}^\dagger \sin kx$ creates an electron inside (outside) L and $\phi_{Y\sigma, \text{in(out)}}^\dagger \sim \int_{x \leq L(x>L)} dx c_{x\sigma}^\dagger \phi_{Y\sigma}(x)$ ($c_{x\sigma}^\dagger$ creates a spin- σ electron at x). $p = \int_L^\infty dx |\phi_Y(x)|^2 \simeq 1/\pi k_Y L \simeq \xi_{1\text{CK}}/\pi L$ is the probability of finding the electron of ϕ_Y outside L . Accordingly, the Fermi sea is written as $|\text{FS}\rangle = \prod_{\substack{k \leq k_F \\ \sigma=\uparrow, \downarrow}} \left(\sqrt{\frac{L}{l}} c_{k\sigma, \text{in}}^\dagger + \sqrt{1 - \frac{L}{l}} c_{k\sigma, \text{out}}^\dagger \right) |0\rangle_{\text{in}} |0\rangle_{\text{out}} \simeq \lim_{l \rightarrow \infty} |0\rangle_{\text{in}} |\text{FS}\rangle_{\text{out}}$, where $|0\rangle_{\text{in(out)}}$ denotes the vacuum state of $x \leq L$ ($x > L$) and $|\text{FS}\rangle_{\text{out}} \equiv \prod_{\substack{k \leq k_F \\ \sigma=\uparrow, \downarrow}} c_{k\sigma, \text{out}}^\dagger |0\rangle_{\text{out}}$ is the Fermi sea outside L . Here, we used $l \gg L$, where the portion of plane waves inside L can be ignored and $|\text{FS}\rangle_{\text{out}}$ is well defined. Using the decomposition, we find

$$|\psi_Y\rangle \simeq \frac{1}{\sqrt{2}} \left[|\uparrow\rangle (\sqrt{1-p} \phi_{Y\downarrow, \text{in}}^\dagger + \sqrt{p} \phi_{Y\downarrow, \text{out}}^\dagger) - |\downarrow\rangle (\sqrt{1-p} \phi_{Y\uparrow, \text{in}}^\dagger + \sqrt{p} \phi_{Y\uparrow, \text{out}}^\dagger) \right] |0\rangle_{\text{in}} |\text{FS}\rangle_{\text{out}}.$$

Then, we compute $\text{Tr}_{x>L} |\psi_Y\rangle \langle \psi_Y| = \sum_i \langle \psi_{i, \text{out}} | \psi_Y \rangle \langle \psi_Y | \psi_{i, \text{out}} \rangle$, where $|\psi_{i, \text{out}}\rangle$'s are relevant states outside L , $|\psi_{i, \text{out}}\rangle \in \{|\text{FS}\rangle_{\text{out}}, \phi_{Y\uparrow, \text{out}}^\dagger |\text{FS}\rangle_{\text{out}}, \phi_{Y\downarrow, \text{out}}^\dagger |\text{FS}\rangle_{\text{out}}\}$. The result is

$$\text{Tr}_{x>L} |\psi_Y\rangle \langle \psi_Y| \simeq (1-p) |\psi_{1, \text{in}}\rangle \langle \psi_{1, \text{in}}| + \frac{p}{2} |\psi_{2, \text{in}}\rangle \langle \psi_{2, \text{in}}| + \frac{p}{2} |\psi_{3, \text{in}}\rangle \langle \psi_{3, \text{in}}|, \quad (\text{S9})$$

where $|\psi_{1, \text{in}}\rangle \equiv \frac{1}{\sqrt{2}} (|\uparrow\rangle \phi_{Y\downarrow, \text{in}}^\dagger - |\downarrow\rangle \phi_{Y\uparrow, \text{in}}^\dagger) |0\rangle_{\text{in}}$, $|\psi_{2, \text{in}}\rangle \equiv |\downarrow\rangle |0\rangle_{\text{in}}$, and $|\psi_{3, \text{in}}\rangle \equiv |\uparrow\rangle |0\rangle_{\text{in}}$.

We calculate $\mathcal{E}_F(\text{Tr}_{x>L} |\psi_Y\rangle \langle \psi_Y|)$, using a witness operator similar to Eq. (3),

$$X_Y = \frac{2}{\log 2} |\psi_{1, \text{in}}\rangle \langle \psi_{1, \text{in}}| - \left(\frac{2}{\log 2} - 1 \right) I_{1, \text{in}}, \quad (\text{S10})$$

where $I_{1, \text{in}} = \sum_{\eta=\uparrow, \downarrow; \sigma=\uparrow, \downarrow} |\eta\rangle \langle \eta| \otimes |\phi_{Y\sigma, \text{in}}\rangle \langle \phi_{Y\sigma, \text{in}}|$ and $|\phi_{Y\sigma, \text{in}}\rangle = \phi_{Y\sigma, \text{in}}^\dagger |0\rangle_{\text{in}}$. This operator is the optimal witness operator for $\mathcal{E}_F(|\psi_{i, \text{in}}\rangle)$ with $i = 1, 2, 3$, namely, it provides the exact value of $\mathcal{E}_F(|\psi_{i=1,2,3, \text{in}}\rangle)$; one checks $\mathcal{E}_F(|\psi_{1, \text{in}}\rangle) = \langle \psi_{1, \text{in}} | X_Y | \psi_{1, \text{in}} \rangle = 1$, $\mathcal{E}_F(|\psi_{2, \text{in}}\rangle) = \mathcal{E}_F(|\psi_{3, \text{in}}\rangle) = 0$. According to the duality [11, 12] between Eqs. (1) and (2), the expectation value of X_Y equals the exact value of \mathcal{E}_F for any mixture of $|\psi_{i=1,2,3, \text{in}}\rangle$ including $\mathcal{E}_F(\text{Tr}_{x>L} |\psi_Y\rangle \langle \psi_Y|)$. We obtain $\mathcal{E}_F(\text{Tr}_{x>L} |\psi_Y\rangle \langle \psi_Y|) = \text{Tr}[X_Y (\text{Tr}_{x>L} |\psi_Y\rangle \langle \psi_Y|)] \simeq 1 - p$, namely, $1 - \mathcal{E}_F(\text{Tr}_{x>L} |\psi_Y\rangle \langle \psi_Y|) \simeq p \propto \xi_{1\text{CK}}/L$. This confirms the universal power law in Eq. (5), which we numerically find in the main text. This computation based on X_Y indicates the usefulness of witness operators for analytically studying macroscopic entanglement EoF in many-body mixed-states.

IX. KONDO CLOUD AT FINITE TEMPERATURE

In Fig. S2, we present our numerical result of the dependence of $\mathcal{E}_F(\rho)$ on L at finite T . Figure S2 shows that as L decreases, \mathcal{E}_F starts to decrease near $L \simeq \xi_{1\text{CK}}$ at $T \lesssim T_{1\text{CK}}$, while roughly near thermal length $L \simeq L_T \equiv \hbar v_F / k_B T$ at $T \gtrsim T_{1\text{CK}}$. This means that the size of Kondo cloud is $\xi_{1\text{CK}}$ and robust against thermal effects at $T \lesssim T_{1\text{CK}}$, while it is roughly L_T , decreasing with increasing T , at $T \gtrsim T_{1\text{CK}}$. Moreover, Fig. S3 suggests that the two 1CK power-law decays in Eqs. (4) and (5) are additive at $T \ll T_{1\text{CK}}$ and $L \gg \xi_{1\text{CK}}$,

$$\mathcal{E}_F \simeq 1 - a_1 \left(\frac{T}{T_{1\text{CK}}} \right)^2 - b_1 \left(\frac{\xi_{1\text{CK}}}{L} \right). \quad (\text{S11})$$

Together with the fact that the two 1CK power laws are not connected by the usual replacement of $k_B T \leftrightarrow \hbar v_F / L$ by the uncertainty relation (as their power-law exponents are different), these unusual findings indicate that the

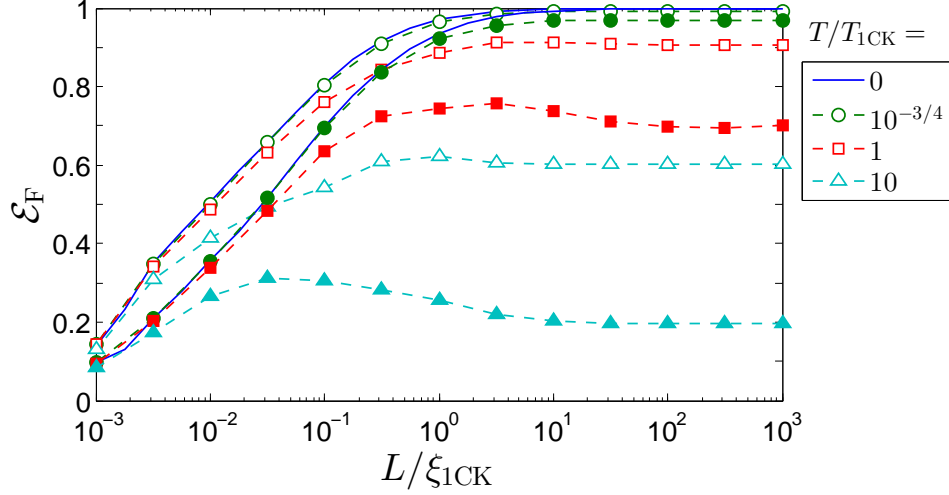


FIG. S2. Kondo cloud at finite temperature. Dependence of EoF \mathcal{E}_F on L at different T 's, $T/T_{1CK} = 0, 10^{-3/4} (\simeq 0.18), 1, 10$; the results of $T/T_{1CK} = 0$ and $10^{-3/4}$ are almost overlapped. This shows that the cloud size is about ξ_{1CK} at $T \lesssim T_{1CK}$, while it decreases at $T \gtrsim T_{1CK}$ as T increases. Empty (filled) symbols represent a upper (lower) bound of \mathcal{E}_F .

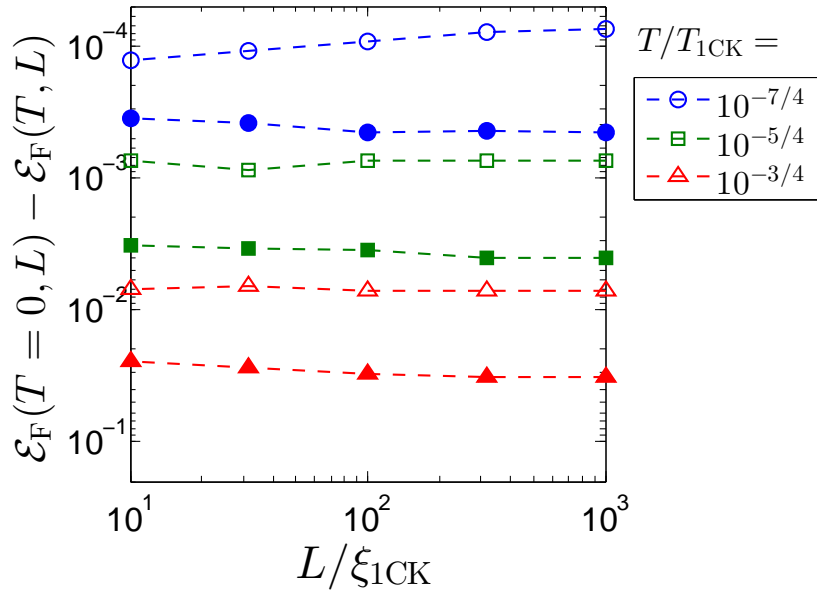


FIG. S3. Dependence of $\mathcal{E}_F(T=0) - \mathcal{E}_F(T)$ on L at different T 's, $T/T_{1CK} = 10^{-3/4} (\simeq 0.18), 10^{-5/4} (\simeq 0.056), 10^{-7/4} (\simeq 0.018)$. This shows that $\mathcal{E}_F(T=0) - \mathcal{E}_F(T)$ is almost independent of L at $T \ll T_{1CK}$ and $L \gg \xi_{1CK}$. Empty (filled) symbols represent a upper (lower) bound of \mathcal{E}_F .

mechanism of entanglement suppression by thermal effects differs from that by the partial trace over $x > L$. Note that we are unable to definitely conclude whether the cloud size is L_T at $T \gtrsim T_{1CK}$, because the numerical results of the upper and lower bounds of \mathcal{E}_F are not close enough to each other; the witness operator X is devised from the entanglement feature of the ground and low-energy eigenstates, hence, less efficient at $T \gtrsim T_{1CK}$ or $L \lesssim \xi_{1CK}$.

All these findings can be understood by the following argument. At finite T , $\mathcal{E}_F(\rho)$ is mainly contributed by the excited states $|E_i\rangle = b_{i\uparrow}|\uparrow\rangle|e_{i\uparrow}\rangle + b_{i\downarrow}|\downarrow\rangle|e_{i\downarrow}\rangle$ of $E_i \sim k_B T$. They have $\mathcal{E}_F(|E_i\rangle) \simeq 1 - 2|S_{z,ii}|^2 / \log 2 = 1 - (|b_{i\uparrow}|^2 - |b_{i\downarrow}|^2)^2 / (2 \log 2)$. For larger E_i , $|S_{z,ii}|^2 \propto (|b_{i\uparrow}|^2 - |b_{i\downarrow}|^2)^2$ increases, as $|E_i\rangle$ more deviates from the exact Bell state. Our numerical results imply that the dependence of \mathcal{E}_F on T reflects this behavior, hence, the entanglement of excited states $|E_i\rangle$. On the other hand, the L dependence of \mathcal{E}_F is related to the loss of the wave functions of

$|e_{i\uparrow}\rangle$ and $|e_{i\downarrow}\rangle$ by the partial trace over $x > L$. At $T \ll T_{\text{1CK}}$ and $L \gg \xi_{\text{1CK}}$, the two mechanisms ($|S_{z,ii}|^2$ and the partial wave-function loss) seem to work independently, resulting in the additive scaling law in Eq. (S11) as $\mathcal{E}_{\text{F}} \simeq (1 - a_1(T/T_{\text{1CK}})^2)(1 - b_1\xi_{\text{1CK}}/L) \simeq 1 - a_1(T/T_{\text{1CK}})^2 - b_1\xi_{\text{1CK}}/L$. The size of Kondo cloud, measured by \mathcal{E}_{F} , may directly reflect the spatial extension of the wave functions $\langle x|e_{i\uparrow}\rangle$ and $\langle x|e_{i\downarrow}\rangle$ participating in excited-state entanglement.
